European Journal of Orthopaedic Surgery & Traumatology (2019) 29:659–666
https://doi.org/10.1007/s00590-018-2322-8

ORIGINAL ARTICLE • KNEE - ARTHROPLASTY

Usefulness of slice encoding for metal artifact correction (SEMAC) technique for reducing metal artifacts after total knee arthroplasty

Ahmed Jawhar[1] · Miriam Reichert[2] · Michael Kostrzewa[4] · Mathias Nittka[3] · Ulrike Attenberger[2] · Henning Roehl[1] · Frederic Bludau[1]

Received: 7 July 2018 / Accepted: 19 September 2018 / Published online: 11 October 2018
© Springer-Verlag France SAS, part of Springer Nature 2018

Abstract

Purpose To evaluate the usefulness of a novel MRI sequence strategy in the assessment of the periprosthetic anatomical structures after primary total knee arthroplasty.

Methods Two MR sequences were retrospectively compared for the imaging of 15 patients with implanted cruciate-retaining/fixed-bearing TKAs (DePuy, PFC Sigma): a slice encoding sequence for metal artifact correction (SEMAC) and a standard sequence. Images were acquired on a 1.5-T system. The degree of artifact reduction was assessed using several qualitative (Likert-type scale) (artifact size, distorsion, blur, image quality, periprosthetic bone, posterior cruciate ligament, lateral collateral ligament, medial collateral ligament, patella tendon, popliteal vessels) and quantitative (artifact volume, Insall–Salvati index, length of patella/tendon, prosthesis dimensions) parameters by blinded reads performed by four investigators. The SEMAC sequences were statistically compared with the standard sequence using Wilcoxon test. Additionally, the intraclass correlation coefficient (ICC) for interobserver agreement was calculated.

Results Higher levels of blurring were found with SEMAC compared to standard sequences ($p < 0.001$). All other qualitative parameters improved significantly with the application of SEMAC. In comparison with conventional sequences, the artifact volume was reduced by 59% utilizing SEMAC. Thus, the artifact reduction improved the precision of measurements such as Insall–Salvati index and length of patella/tendon ($p < 0.001$). The dimension of the tibial component (Ti alloy/polyethylene) revealed accurate values with both MRI sequences. A sufficient interobserver agreement among all readers was found with SEMAC, qualitatively ICC 0.9 (range 0.8–1) as well as quantitatively ICC 0.95 (range 0.92–0.98).

Conclusions SEMAC effectively reduces artifacts caused by metallic implants after total knee arthroplasty relative to standard imaging. This allows for an improved assessment of periprosthetic anatomical structures. This might enable an improved detectability of postoperative complications in the future.

Level of evidence Diagnostic Study Level III.

Keywords Total knee arthroplasty · Ligaments · Periprosthetic bone · SEMAC · Artifact reduction

Introduction

The long-term success after primary total knee arthroplasty (TKA) depends on patient selection and surgical technique ensuring an accurate implant positioning with balanced soft tissue [17]. Despite efforts to improve surgical techniques, 20% of patients worldwide remain dissatisfied with their results after primary TKA due to substantial pain [16]. Thirty-five percentage of early TKA revisions are performed due to unbalanced or insufficient periprosthetic soft tissue [5]. The unbalanced soft tissue in turn could clinically explain anterior knee pain, stiffness/instability [20], recurrent effusion [15] and early component loosing [3]. The number of TKA revisions is estimated to grow significantly until 2030 [7]. The diagnosis leading to revision surgery is usually based on native radiographs/CT scans/bone scintigraphy and the subjective clinical orthopedic examination [12]. To clarify the etiology of the symptoms after primary TKA more accurately, MR imaging might be useful,

Henning Roehl and Frederic Bludau have contributed equally to this work.

✉ Ahmed Jawhar
Ahmed.Jawhar@umm.de

Extended author information available on the last page of the article

especially in cases with synovitis, periprosthetic osteolysis, fractures, tendon/muscle injuries, instability, arthrofibrosis and mechanical component damages [18].

However, the efficiency of standard MR imaging for the evaluation of the periprosthetic tissues is limited due to susceptibility artifacts of the implant components, which consecutively contributes to poor-quality images. Therefore, MR imaging has not been routinely used in the presence of knee endoprosthesis [10].

Recently, numerous MR imaging strategies were introduced and evolved to reduce metal artifacts. The SEMAC sequence, which has been previously described in detail [9, 14], corrects both in-plane and through-plane metal-implant-induced artifacts [9]. The SEMAC technique effectively reduced artifacts generated by different implants compared to conventional imaging at 1.5 T [14].

However, the limited data [1, 2, 19] did not provide a solid base for clinical decision making: whether the SEMAC technique is useful for human imaging of periprosthetic tissue in the presence of highly paramagnetic TKAs.

To our knowledge, the present study is the first one assessing the usefulness of the SEMAC technique in primary, cruciate-retaining, fixed-bearing TKA (DePuy, PFC Sigma).

The aim of the present study was to compare SEMAC with standard sequences concerning the qualitative and quantitative assessments of the periprosthetic tissue after primary TKA.

Patients and methods

The present retrospective study was carried out in accordance with the Declaration of Helsinki. Retrospective MR data analysis was approved by our Institutional Ethics Committee (file reference 2008-338N-MA).

Patients suffering from unspecific postoperative knee symptoms after TKA were scheduled to undergo MRI with SEMAC and standard sequences at the end stage of their routine clinical workup.

Fifteen patients (11 females and 4 males) with a mean age of 76 years (range 52–89 years) with complete data sets were included in the retrospective study. They underwent TKA from 12 to 24 months prior to MR imaging.

Patients had received a cemented (SmartSet Bone cement, DePuy/Synthes, Warsaw, IN, USA) fixed-bearing, cruciate-retaining TKA (DePuy, PFC Sigma). The femoral component consists of CoCrMo alloy, whereas the tibial plateau consists of Ti alloy and a polyethylene insert.

MR imaging technique

Patients were placed supine on the MRI table. A 1.5-T MRI scanner (MAGNETOM Avanto, Siemens Healthcare, Erlangen, Germany) was used for all cases. The MR imaging protocol applied T1 coronar, T2 transversal and PD sagittal sequences. SEMAC imaging was performed with a prototype software package (Siemens Healthcare, Erlangen, Germany), providing a 2D TSE sequence with View Angle Tilting (VAT), Slice Encoding for Metal Artifact correction (SEMAC), and optimized for high-bandwidth imaging parameters. A standard 2D TSE sequence served as a reference. The details of the image parameters are described in Table 1.

Qualitative analysis of the MRI

The MR images from the knee joints were retrospectively assessed independently by a total of four readers. Two experienced orthopedic surgeons and two experienced diagnostic radiologists evaluated the images. The readers were not aware of the sequence type at the time of evaluation/measurement.

Images with SEMAC and standard sequences were compared qualitatively side by side and with the same contrast according to defined qualitative parameters: artifact size; image distorsion; image blur; visualization of the bone marrow/bone cortex/soft tissue; posterior cruciate ligament, lateral collateral ligament, medial collateral ligament, patella tendon, popliteal vessels, periprosthetic bone (Figs. 1, 2, 3, 4). The images were graded as described (Tables 2, 3).

Table 1 Image parameter at 1.5 T

	T1		T2		PD	
	Standard	SEMAC	Standard	SEMAC	Standard	SEMAC
TR (ms)	512	650	5310	3300	3000	4570
TE (ms)	11	6	79	74	14	36
Readout BW (kHz/pixel)	150	651	189	651	127	651
Matrix	320×300	320×256	320×256	320×256	256×256	320×256
Slice thickness (mm)	3	2	3	4	3	2
Acquisition time (min:s)	04:09	11:22	04:32	11:31	2:28	3:17

TR repetition time, *TE* echo time, *BW* readout bandwidth, *PD* proton density

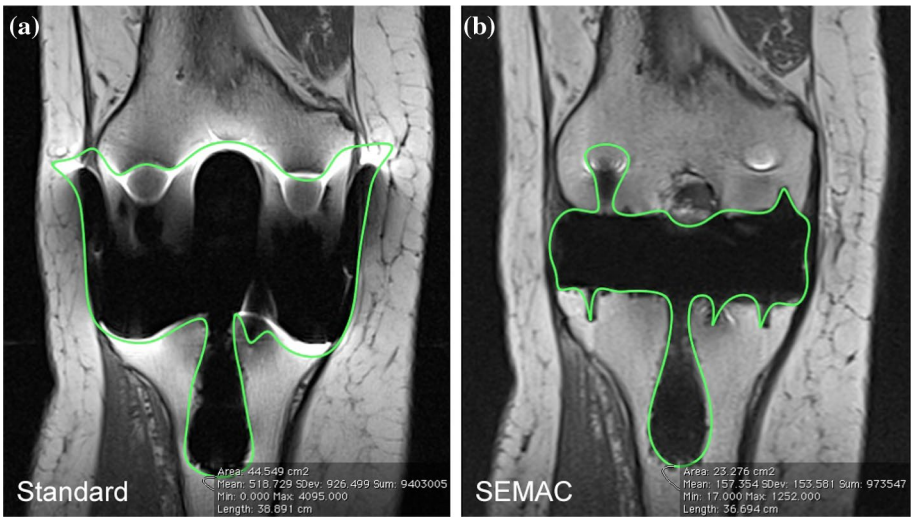

Fig. 1 Measurement of periprosthetic artifact volume after **a** standard and **b** SEMAC sequence MRI

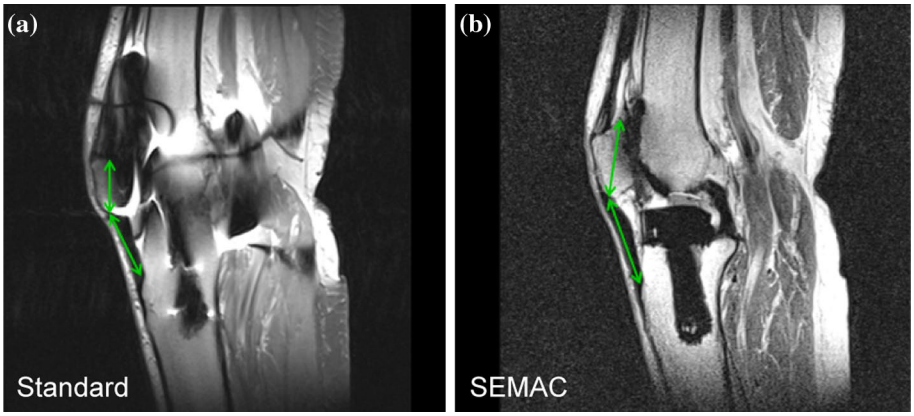

Fig. 2 Measurement of the patella height with **a** standard and **b** SEMAC sequence using the formula: Insall–Salvati index = length of patella tendon/diagonal length of patella. The identification of several periprosthetic anatomical landmarks such as quadriceps tendon, patella, patella tendon, tibial tuberosity, posterior cruciate ligament is markedly improved with SEMAC

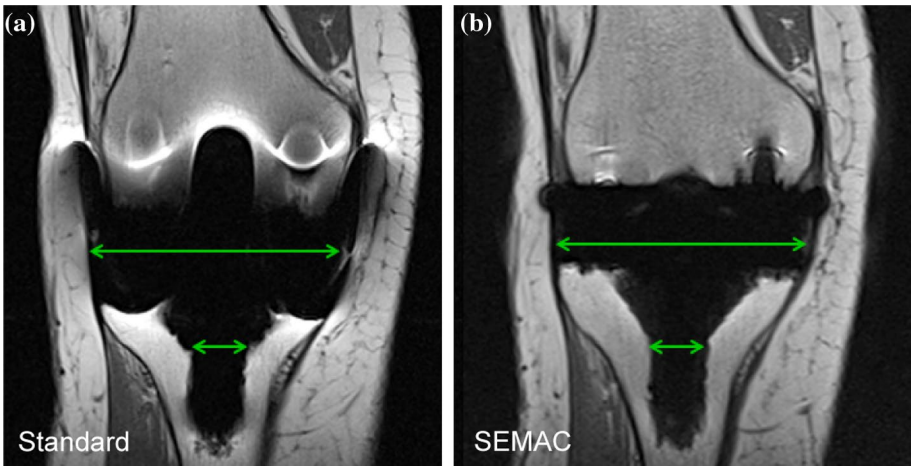

Fig. 3 Measurement of mediolateral tibia plateau and tibia stem width with sagittal **a** standard and **b** SEMAC sequences

Quantitative analysis of the MRI

The artifact volume generated by the implant components was measured by an experienced radiologist (Fig. 1). The artifact volume was determined offline using a dedicated workstation (GE Healthcare, Advantage Workstation AW4.2, Erlangen, Germany). The reliable method of artifact volume quantification first described by Lee et al. [8] was utilized for the analysis of each sequence.

Four readers independently compared SEMAC and standard sequence images side by side and with the same contrast according to defined quantitative parameters: Insall–Salvati

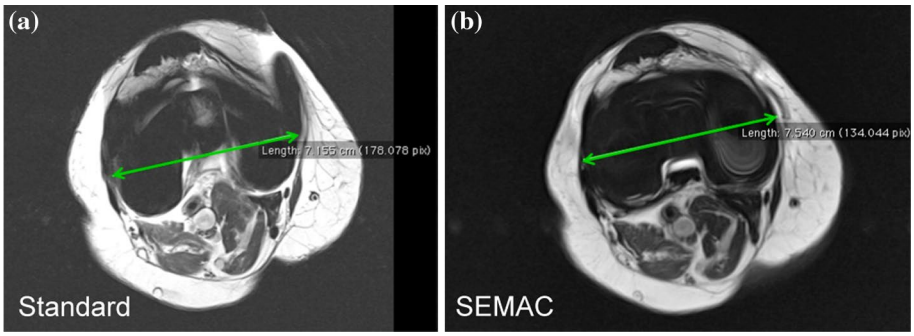

Fig. 4 Measurement of mediolateral tibia plateau and tibia stem width with transversal **a** standard and **b** SEMAC sequences

Table 2 Overall qualitative evaluation between MR imaging modalities by four readers for the metal artifact reduction

[a]	Surgeon 1		Surgeon 2		Radiologist 1		Radiologist 2		Reliability (ICC)	
	Standard	SEMAC	Standard	SEMAC	Standard	SEMAC	Standard	SEMAC	Standard	SEMAC
Artifact size										
Mean	2.0	1.0	2.0	1.0	2.0	1.0	2.0	1.0	1	1
SD	0.0	0.0	0.0	0.0	0.0	0.0	0.0	0.0		
p value		< 0.001		< 0.001		< 0.001		< 0.001	< 0.001	< 0.001
Imaging distortion										
Mean	2.0	1.0	2.0	1.0	2.0	1.0	2.0	1.0	1	1
SD	0.0	0.0	0.0	0.0	0.0	0.0	0.0	0.0		
p value		< 0.001		< 0.001		< 0.001		< 0.001	< 0.001	< 0.001
Imaging blur										
Mean	1.1	1.9	1.1	1.9	1.0	2.0	1.0	2.0	0.80	0.80
SD	0.3	0.3	0.3	0.3	0.0	0.0	0.0	0.0		
p value		< 0.001		< 0.001		< 0.001		< 0.001	< 0.001	< 0.001
Visualization of bone marrow/bone cortex and soft tissue										
Mean	1.9	1.1	2.0	1.0	2.0	1.0	2.0	1.0	0.95	0.95
SD	0.3	0.3	0.0	0.0	0.0	0.0	0.0	0.0		
p value		< 0.001		< 0.001		< 0.001		< 0.001	< 0.001	< 0.001
Overall image quality										
Mean	2.0	1.0	2.0	1.0	2.0	1.0	2.0	1.0	1	1
SD	0.0	0.0	0.0	0.0	0.0	0.0	0.0	0.0		
p value		< 0.001		< 0.001		< 0.001		< 0.001	< 0.001	< 0.001

[a] 1 = best; 2 = worst

index [11], length of patella, length of patella tendon, diameter of tibial stem, medial–lateral width of the tibia plateau (Figs. 2, 3, 4; Table 4).

Statistical analysis

Statistical analysis was performed using commercial statistical software package (SPSS for Windows, version 23). The results are presented with mean ± standard deviation (SD). Nonparametric Wilcoxon test was used for the statistical comparison among different imaging protocols. As evaluated by four readers, intraclass correlation coefficient (ICC) was used to calculate the interobserver agreement for the SEMAC and standard sequences separately. A $p < 0.05$ was set to be statistically significant.

Results

Qualitative analysis of the MRI

Increased blurring was noted with SEMAC compared to standard sequences. A statistically significant superiority of SEMAC was found for all other qualitative parameters (artifact size, distortion, image quality, periprosthetic bone, posterior cruciate ligament, lateral collateral ligament, medial collateral ligament, patella tendon, popliteal vessels (all $p < 0.001$).

Table 3 Qualitative evaluation between MR imaging modalities by four readers with regard to identification of clinically relevant structures

[a]	Surgeon 1		Surgeon 2		Radiologist 1		Radiologist 2		Reliability (ICC)	
	Standard	SEMAC	Standard	SEMAC	Standard	SEMAC	Standard	SEMAC	Standard	SEMAC
PCL										
Mean	3.0	1.2	3.0	1.0	2.9	1.0	2.9	1.0	0.90	0.90
SD	0.0	0.4	0.0	0.0	0.3	0.0	0.3	0.0		
p value		< 0.001		< 0.001		< 0.001		< 0.001	< 0.001	< 0.001
MCL										
Mean	2.7	1.3	2.1	1.1	2.0	1.3	2.1	1.2	0.34	0.80
SD	0.5	0.6	0.3	0.3	0.0	0.4	0.3	0.4		
p value		< 0.001		< 0.001		< 0.001		< 0.001	0.6	< 0.001
LCL										
Mean	2.2	1.4	2.1	1.3	2.0	1.3	2.1	1.3	0.37	0.87
SD	0.4	0.5	0.3	0.4	0.0	0.4	0.3	0.4		
p value		< 0.001		< 0.001		< 0.001		< 0.001	0.16	< 0.001
Patella tendon										
Mean	2.1	1.1	1.9	1.0	1.9	1.0	1.9	1.0	0.68	0.99
SD	0.5	0.3	0.3	0.0	0.3	0.0	0.3	0.0		
p value		< 0.001		< 0.001		< 0.001		< 0.001	< 0.001	< 0.001
Popliteal vessels										
Mean	2.2	1.1	1.5	1.1	1.4	1.2	1.5	1.2	0.83	0.87
SD	0.6	0.3	0.5	0.3	0.5	0.4	0.6	0.4		
p value		< 0.001		< 0.001		< 0.001		< 0.001	< 0.001	< 0.001
Periprosthetic bone										
Mean	2.0	1.0	2.0	1.0	2.0	1.2	2.0	1.1	1.0	0.80
SD	0.0	0.0	0.0	0.0	0.0	0.4	0.0	0.3		
p value		< 0.001		< 0.001		< 0.001		< 0.001	< 0.001	< 0.001

[a] 1 = completely visible; 2 = partially visible; 3 = not visible

Mean ICC was 0.9 (range 0.8–1) for the SEMAC sequences and 0.8 (range 0.34–1) for the standard sequences (Tables 2, 3).

Quantitative analysis of the MRI

In comparison with the standard method, the artifact volume was reduced significantly by 59% with SEMAC sequences ($p < 0.001$) (Fig. 5). With the reduction in the artifact volumes, the precision of the measurements such as Insall–Salvati index and length of patella/tendon improved. The mediolateral width of the tibial component, which consists of a Ti alloy/polyethylene insert, revealed accurate measurement values with both methods as compared to real dimensions provided by the manufacturer. The mean ICC of the SEMAC sequence was 0.95 (range 0.92–0.98). The ICC of the standard sequence averaged 0.85 (range 0.72–0.92; Table 4).

Discussion

The principal finding of the present study was that SEMAC sequence MRI successfully reduced the artifact volume and thus improved the quantitative/qualitative evaluation of periprosthetic tissue after primary TKA.

Sutter et al. [19] implanted a different prosthesis design/manufacturer and described a significant reduction in artifact size with SEMAC. Similar to previously published studies [1, 14], we found increased blurring with SEMAC compared to standard sequences.

The results of the present study suggest that MR imaging with SEMAC allows for adequate identification and evaluation of the collateral ligaments as well as PCL. Failing to obtain balanced periprosthetic ligaments or to retain the PCL in corresponding prosthesis designs results

Table 4 Quantitative comparison between MR imaging modalities by four readers with regard to measurement of clinically relevant parameter

	Surgeon 1		Surgeon 2		Radiologist 1		Radiologist 2		Reliability (ICC)	
	Standard	SEMAC	Standard	SEMAC	Standard	SEMAC	Standard	SEMAC	Standard	SEMAC
Insall–Salvati index[a]										
Mean	0.79	1.01	0.80	1.05	0.97	1.13	0.87	1.11	0.72	0.93
SD	0.1	0.2	0.1	0.1	0.1	0.2	0.1	0.2		
p value		< 0.001		< 0.001		< 0.001		< 0.001	< 0.001	< 0.001
Length of patella (mm)										
Mean	42.0	40.2	44.1	39.1	41.3	36.9	42.0	37.7	0.92	0.92
SD	13.8	3.5	8.9	2.9	9.0	3.5	6.9	3.8		
p value		> 0.05		< 0.05		< 0.05		< 0.05	< 0.001	< 0.001
Length of patella tendon (mm)										
Mean	31.8	40.0	32.5	40.2	37.9	40.7	36.5	41.1	0.79	0.98
SD	10.0	6.0	3.7	5.7	6.2	6.3	7.0	6.5		
p value		< 0.001		< 0.001		< 0.05		< 0.001	< 0.001	< 0.001
Tibial stem diameter[b] *(mm)*										
Mean	15,8	14.8	15.8	16.4	16.5	16.9	16.7	16.4	0.92	0.94
SD	1,7	4.4	2.1	1.4	1.6	2.0	1.5	1.6		
p value		> 0.05		> 0.05		> 0.05		> 0.05	< 0.001	< 0.001
Width of tibia plateau[c] *(mm)*										
Mean	71.2	73.0	71.0	71.5	72.2	71.5	72.5	72.1	0.92	0.97
SD	4.9	3.4	3.2	3.2	5.1	3.2	3.1	3.6		
p value		> 0.05		> 0.05		> 0.05		> 0.05	< 0.001	< 0.001

[a]Insall–Salvati index as determined on standard radiographs averaged 1.02 ± 0.2

[b]Tibial stem diameter measured intraoperatively averaged 15.3 ± 0.7 mm

[c]Width of tibia plateau measured intraoperatively averaged 70.5 ± 3 mm

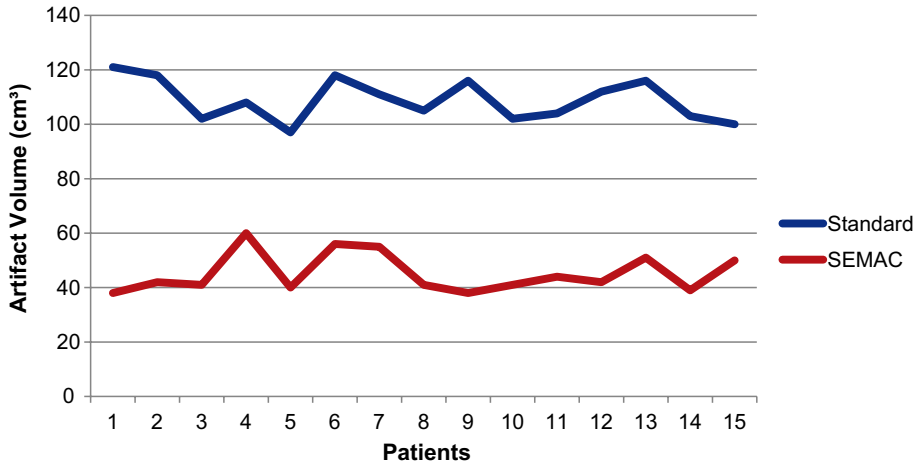

Fig. 5 Comparison of the artifact volume in each case between **a** standard and **b** SEMAC sequences

in early instability, anterior knee pain and revision surgery [20]. Also posttraumatic/degenerative tear of MCL, LCL, PCL or patella tendon could occur after primary TKA [13]. In cases of instability or insufficiency of the extensor mechanism, the visualization of the periprosthetic soft tissue complimentary to the subjective clinical findings might help the orthopedic surgeon to establish the therapeutic management more precisely.

Similar to postoperative radiographic measurements, Insall–Salvati index [11], length of patella and length of patella tendon were detected and measured reliably with SEMAC sequences. The etiology behind patellar height changes with reduced range of movement after TKA remained unknown. Several prominent explanation models exist, e.g., scar tissue/new bone formation, intratendinous fibrosis, tendon adhesion to infrapatellar bursa or proximal

part of tibia, trauma and ischemia [6, 21]. Metal-artifact-reduced MR imaging could be useful to increase understanding about the etiology of patella tendon shrinking/elongation and to accurately quantify the changes of patellar height.

The detection and quantification of periprosthetic osteolysis around TKA with native radiographs were reported to be inferior due to the projection of the implant components on the periprosthetic bone [22].

SEMAC sequences have been proposed to be included in the diagnostic algorithm of patients with a painful TKA, since the detection of clinically relevant periprosthetic osteolysis significantly improved [19].

In summary, MR imaging with SEMAC sequence provided promising detailed diagnostic information about all periprosthetic tissues. The improved characterization and depiction of the periprosthetic anatomical structures due to reduced artifact might contribute to a more reliable and conclusive diagnosis prior to revision surgeries.

The most important limitations of SEMAC sequences are the increased acquisition time (delta 15 min) with consecutively possible patient discomfort and motion artifacts. However, recent data suggest the possibility to reduce the acquisition time by using compressed sensing SEMAC [4]. Residual artifacts sometimes limit a detailed evaluation of bone–cement and cement–metal interfaces.

Future studies with higher sample sizes are required to elucidate the diagnostic value of SEMAC sequences to detect further clinically relevant parameters such as implant position, polyethylene wear, osteolysis, fracture, infection and mechanical complications.

Conclusion

SEMAC effectively reduces artifacts caused by metallic implants after total knee arthroplasty relative to standard imaging. This might allow for an improved detectability of complications after TKA.

Compliance with ethical standards

Conflict of interest Mathias Nittka is an employee of Siemens Healthcare GmbH. The remaining authors declare that there were no conflicts of interest.

References

1. Agten CA, Del Grande F, Fucentese SF, Blatter S, Pfirrmann CW, Sutter R (2015) Unicompartmental knee arthroplasty MRI: impact of slice-encoding for metal artefact correction MRI on image quality, findings and therapy decision. Eur Radiol 25:2184–2193
2. Bachschmidt TJ, Sutter R, Jakob PM, Pfirrmann CW, Nittka M (2015) Knee implant imaging at 3 Tesla using high-bandwidth radiofrequency pulses. J Magn Reson Imaging 41:1570–1580
3. Berend ME, Ritter MA, Meding JB, Faris PM, Keating EM, Redelman R, Faris GW, Davis KE (2004) Tibial component failure mechanisms in total knee arthroplasty. Clin Orthop Relat Res 428:26–34
4. Fritz J, Ahlawat S, Demehri S, Thawait GK, Raithel E, Gilson WD, Nittka M (2016) Compressed sensing SEMAC: 8-fold accelerated high resolution metal artifact reduction MRI of cobalt-chromium knee arthroplasty implants. Invest Radiol 51:666–676
5. Gustke KA, Golladay GJ, Roche MW, Elson LC, Anderson CR (2014) A new method for defining balance: promising short-term clinical outcomes of sensor-guided TKA. J Arthroplasty 29:955–960
6. Jawhar A, Sohoni S, Shah V, Scharf HP (2014) Alteration of the patellar height following total knee arthroplasty. Arch Orthop Trauma Surg 134:91–97
7. Kurtz S, Ong K, Lau E, Mowat F, Halpern M (2007) Projections of primary and revision hip and knee arthroplasty in the United States from 2005 to 2030. J Bone Joint Surg Am 89:780–785
8. Lee MJ, Janzen DL, Munk PL, MacKay A, Xiang QS, McGowen A (2001) Quantitative assessment of an MR technique for reducing metal artifact: application to spin-echo imaging in a phantom. Skeletal Radiol 30:398–401
9. Lu W, Pauly KB, Gold GE, Pauly JM, Hargreaves BA (2009) SEMAC: slice encoding for metal artifact correction in MRI. Magn Reson Med 62:66–76
10. Math KR, Zaidi SF, Petchprapa C, Harwin SF (2006) Imaging of total knee arthroplasty. Semin Musculoskelet Radiol 10:47–63
11. Meneghini RM, Ritter MA, Pierson JL, Meding JB, Berend ME, Faris PM (2006) The effect of the Insall–Salvati ratio on outcome after total knee arthroplasty. J Arthroplasty 21:116–120
12. Mont MA, Serna FK, Krackow KA, Hungerford DS (1996) Exploration of radiographically normal total knee replacements for unexplained pain. Clin Orthop Relat Res 331:216–220
13. Montgomery RL, Goodman SB, Csongradi J (1993) Late rupture of the posterior cruciate ligament after total knee replacement. Iowa Orthop J 13:167–170
14. Reichert M, Ai T, Morelli JN, Nittka M, Attenberger U, Runge VM (2015) Metal artefact reduction in MRI at both 1.5 and 3.0 T using slice encoding for metal artefact correction and view angle tilting. Br J Radiol 88:20140601
15. Schnurr C, Eysel P, Konig DP (2012) Is the effect of a posterior cruciate ligament resection in total knee arthroplasty predictable? Int Orthop 36:83–88
16. Schulze A, Scharf HP (2013) Satisfaction after total knee arthroplasty. Comparison of 1990–1999 with 2000–2012. Orthopade 42:858–865
17. Seon JK, Song EK, Park SJ, Lee DS (2011) The use of navigation to obtain rectangular flexion and extension gaps during primary total knee arthroplasty and midterm clinical results. J Arthroplasty 26:582–590
18. Sofka CM, Potter HG, Figgie M, Laskin R (2003) Magnetic resonance imaging of total knee arthroplasty. Clin Orthop Relat Res 406:129–135
19. Sutter R, Hodek R, Fucentese SF, Nittka M, Pfirrmann CW (2013) Total knee arthroplasty MRI featuring slice-encoding for metal artifact correction: reduction of artifacts for STIR and proton density-weighted sequences. AJR Am J Roentgenol 201:1315–1324
20. Takahashi T, Wada Y, Yamamoto H (1997) Soft-tissue balancing with pressure distribution during total knee arthroplasty. J Bone Joint Surg Br 79:235–239
21. Weale AE, Murray DW, Newman JH, Ackroyd CE (1999) The length of the patellar tendon after unicompartmental and total knee replacement. J Bone Joint Surg Br 81:790–795
22. Zotti MG, Campbell DG, Woodman R (2012) Detection of periprosthetic osteolysis around total knee arthroplasties an in vitro study. J Arthroplasty 27:317–322

Affiliations

Ahmed Jawhar[1] · Miriam Reichert[2] · Michael Kostrzewa[4] · Mathias Nittka[3] · Ulrike Attenberger[2] · Henning Roehl[1] · Frederic Bludau[1]

Miriam Reichert
Miriam.Reichert@medma.uni-heidelberg.de

Michael Kostrzewa
michael.kostrzewa@uhn.ca

Mathias Nittka
mathias.nittka@siemens.com

Ulrike Attenberger
Ulrike.Attenberger@umm.de

Henning Roehl
Henning.roehl@diakonissen.de

Frederic Bludau
Frederic.bludau@umm.de

[1] Department of Orthopaedics and Trauma Surgery, University Medical Center Mannheim, Medical Faculty Mannheim, Heidelberg University, Theodor-Kutzer-Ufer 1-3, 68167 Mannheim, Germany

[2] Department of Clinical Radiology and Nuclear Medicine, Institute of Clinical Radiology and Nuclear Medicine, University Medical Center Mannheim, Medical Faculty Mannheim, Heidelberg University, Theodor-Kutzer-Ufer 1-3, 68167 Mannheim, Germany

[3] Siemens Healthcare GmbH, Allee am Roethelheimpark 2, 91052 Erlangen, Germany

[4] Division of Vascular and Interventional Radiology, Department of Medical Imaging, Toronto General Hospital and Mount Sinai Hospital, University of Toronto, NCSB 1C-568, 585 University Ave., Toronto, ON M5G 2N2, Canada